



CHORUS

This is the accepted manuscript made available via CHORUS. The article has been published as:

Temperature dependence of spin-orbit torques in Cu-Au alloys

Yan Wen, Jun Wu, Peng Li, Qiang Zhang, Yuelei Zhao, Aurelien Manchon, John Q. Xiao, and Xixiang Zhang

Phys. Rev. B **95**, 104403 — Published 6 March 2017

DOI: [10.1103/PhysRevB.95.104403](https://doi.org/10.1103/PhysRevB.95.104403)

Temperature dependence of spin orbit torques in Cu Au alloys

Yan Wen¹, Jun Wu², Peng Li¹, Qiang Zhang¹, Yuelei Zhao¹, Aurelien Manchon^{1,‡}, John Q. Xiao^{2,†} and Xixiang Zhang^{1,*}

¹King Abdullah University of Science and Technology (KAUST), Physical Science and Engineering Division (PSE), Thuwal 23955 6900, Saudi Arabia

²University of Delaware, Department of Physics and Astronomy, Newark, Delaware 19716, USA

Abstract

We investigated current driven spin orbit torques in $\text{Cu}_{40}\text{Au}_{60}/\text{Ni}_{80}\text{Fe}_{20}/\text{Ti}$ layered structures with in-plane magnetization. We have demonstrated a reliable and convenient method to separate dampinglike torque and fieldlike torque by using the second harmonic technique. It is found that the dampinglike torque and fieldlike torque depend on temperature very differently. Dampinglike torque increases with temperature while fieldlike torque decreases with temperature, which are different from results obtained previously in other material system. We observed a nearly linear dependence between the spin Hall angle and longitudinal resistivity, suggesting that skew scattering may be the dominant mechanism of spin orbit torques.

[‡]Aurelien.Manchon@kaust.edu.sa

[†]jqx@udel.edu

^{*}xixiang.zhang@kaust.edu.sa

1 **Introduction:**

2 Bulk materials and/or interfaces with large spin orbit coupling
3 have attracted significant attention recently, since they can generate
4 substantial spin current or spin accumulation that can be used to
5 manipulate the magnetic moment [1-8]. When spin current is generated
6 by non magnetic (NM) layer via the spin Hall effect (SHE), the
7 accumulated spins can diffuse into the ferromagnetic (FM) layer and
8 interact with the magnetic moment of the FM layer via spin transfer
9 torque. Spin accumulation can also be generated electrically at the
10 NM/FM interface via the Rashba effect [5,9]. It has been theoretically
11 predicted that both the Rashba effect at the NM/FM interface and the
12 spin Hall effect in the bulk of the NM layer generate dampinglike torque
13 and fieldlike torque upon magnetization [10]. Some recent theories also
14 suggested that spin swapping can contribute to spin orbit torque (SOT)
15 [11].

16 The physics underlying SOT can be investigated when
17 dampinglike torque and fieldlike torque are separated. Recently, second
18 harmonic voltage measurements [12] were used to evaluate the effective
19 field induced by dampinglike torque and fieldlike torque [6,13-18]. This
20 technique has been widely used to characterize SOT in magnetic
21 heterostructures that possess out of plane magnetization and/or have a
22 significant perpendicular magnetic anisotropy. Therefore, a similar
23 electrical measurement technique is needed to characterize the systems
24 with in-plane magnetization [15,17,19,20].

25 The study of the temperature dependence of SOTs is important
26 because it can provide useful information about the physics and
27 mechanisms of SOTs. An accurate understanding of the physics of SOTs
28 is crucial to the efficient structural design of SOT devices. Qiu et al. [21]
29 reported that fieldlike torque decreased linearly with decreasing
30 temperature in Ta/CoFeB/MgO samples, whereas the dampinglike
31 torque mostly remained unaffected. The two different dependences
32 suggest that scattering events involving magnons and phonons play
33 different roles in the two torque components. However, most previous

1 studies focused on Ta [21,22] or Pt based materials in which intrinsic
2 SHE dominates [23,24].

3 In this study, we used a technique to characterize SOTs in
4 materials with in-plane magnetization by modifying the technique
5 previously used on materials with perpendicular magnetization. Using
6 this technique, we studied the SOTs in CuAu/NiFe heterostructures as a
7 function of NM layer thickness and temperature. It was found that both
8 fieldlike torque and dampinglike torque increased monotonically with
9 the thickness of the non magnetic underlayer, as explained by a simple
10 drift diffusion model [25]. However, the dampinglike torque and the
11 fieldlike torque exhibited different temperature behaviors, suggesting
12 that SOT is driven by extrinsic scattering events in this system.

13

14 **Harmonic Response Model:**

15 It is now well known that an in-plane current flowing through a
16 NM/FM heterostructure with strong spin orbit coupling can generate two
17 different SOTs: dampinglike torque, $\sim \bar{m} \times (\bar{\sigma} \times \bar{m})$, and fieldlike torque,
18 $\sim \bar{m} \times \bar{\sigma}$, where \bar{m} is the normalized magnetization vector and $\bar{\sigma}$ is the
19 accumulated spin direction. To calculate the magnetization direction
20 (θ_m, φ_m) , we look for the minimum energy states by considering the
21 anisotropy energy and the Zeeman energy [17] (see Appendix). After an
22 alternative current, $i = I \sin(\omega t)$, is injected, the Hall resistance, $R(t)$,
23 oscillates at the same frequency. The Hall voltage, $V(t) = R(t) I \sin(\omega t)$,
24 thus gives information about the current induced fields. It can also be
25 separated into two parts based on their frequency (see Appendix):

$$26 \quad V_H = \left[R_p \sin 2\varphi_m \sin \omega t + (\Delta\varphi \cdot 2R_p \cos 2\varphi_m - \Delta\theta \cdot R_A) \sin^2 \omega t \right] I, \quad (1)$$

27 where R_A and R_p are the coefficients of the anomalous Hall effect (AHE)
28 and the planer Hall effect (PHE), respectively; $\Delta\theta, \Delta\varphi$ is the change in the
29 polar and azimuthal angles of magnetization under current induced fields,
30 θ_m, φ_m are the polar and azimuthal angles of magnetization in sphere

1 coordinates. We define $\theta=0$ is the direction perpendicular to the film
 2 plane and $\varphi=0$ is the direction parallel to current. The second order term
 3 can be separated out as

$$4 \quad V_{2\omega} = \left(-\Delta\varphi \cdot R_p \cos 2\varphi_m + \frac{1}{2} \Delta\theta \cdot R_A \right) I . \quad (2)$$

5 If the external magnetic field applied in the film plane ($\theta_H = \pi/2$) is strong
 6 enough to keep the magnetic moment almost in-plane ($\theta_m \cong \pi/2$), we can
 7 obtain the following equation:

$$8 \quad V_{2\omega} = \left(\frac{-H_{FL} \cos \varphi}{H - H_A} \cdot R_p \cos 2\varphi + \frac{1}{2} \frac{H_{DL} \cos \varphi}{H_K - H} \cdot R_A \right) I , \quad (3)$$

9 where H_K and H_A are the effective out of plane and in-plane anisotropy
 10 field, respectively. Given the above relations, a larger external field
 11 significantly decreases the second order voltage. To overcome this
 12 problem, we choose some optimized fields that can both fulfill the
 13 approximation requirement and obtain strong and measurable signals.
 14 By scanning the angle of the external field in-plane, the effective fields
 15 induced by fieldlike torque and dampinglike torque can be obtained.

16

17 **Experimental details**

18 $\text{Cu}_{40}\text{Au}_{60}/\text{Ni}_{80}\text{Fe}_{20}/\text{Ti}$ layered structures were fabricated on SiO_2/Si
 19 substrates at room temperature using sputtering. Electrical transport
 20 properties and magnetic properties of the samples were characterized
 21 over a wide temperature ranging from 20 K to 300 K under different
 22 magnetic fields. SOTs were measured by the second harmonic Hall
 23 voltage method. An AC voltage of 5 volts with a frequency of 87.34 Hz
 24 was applied using an SR830 Locked in Amplifier.

25

1 Results and discussion

2 Shown in Fig. 1(a) is the schematic of the measurement setup for
 3 CuAu (8)/ NiFe (1.5)/ Ti (1) (thickness in nanometers) samples. Fig. 1(b)
 4 shows the first harmonic voltage, V_ω , as a function of the azimuthal
 5 angle, φ , measured under a magnetic field, $H=50$ Oe, at different
 6 temperatures (20 to 300 K). To obtain the coefficient of the planar Hall
 7 effect, R_p , we fitted the data to $V_\omega = R_p \sin 2\varphi_m \cdot I$. We note that R_p is
 8 independent of the field at higher fields and that the data follow $\sin 2\varphi$
 9 dependence very well, indicating that the moment is always along with
 10 the external field even at 50 Oe, i.e. anisotropy field $|H_A| < 50$ Oe. Close
 11 analysis reveals that $|H_A| \sim 10$ Oe. A slight shape deviation and a decrease
 12 in R_p with increasing temperature are observed at this field. The
 13 dependence of Hall resistance on perpendicular external fields obtained
 14 at different temperatures is shown in Fig. 1(c). The nearly linear
 15 dependence of Hall effect on the magnetic field and the very small
 16 coercive field (< 50 Oe) indicate clearly that the magnetization is lying
 17 in the film plane and the perpendicular magnetic anisotropy is very weak.
 18 In this case, the Hall effect will saturate at the magnetic fields being
 19 equal to the demagnetization fields at different temperatures. The
 20 demagnetizing field varies from about 5 kOe to 7 kOe as the temperature
 21 decreases from 300 K to 20 K, which is ascribed to the temperature
 22 dependent saturation magnetization. To gain a deeper understanding of
 23 the magnetic properties of the bilayers, we carefully studied the
 24 magnetization as a function of temperature and field. Fig. 1(d) shows the
 25 in-plane magnetization versus magnetic field curves (up to ± 1 T)
 26 measured at various temperatures between 20 K and 300 K. A magnetic
 27 field of 0.5 T is required to saturate the magnetization as M_s decreases
 28 linearly with temperature, rather than following Bloch's $T^{3/2}$ law due to
 29 the two dimensional nature of the samples. The temperature dependence
 30 of saturation magnetization $M_s(T)$, is useful in understanding the
 31 dependence of the spin Hall angle on temperature.

1 The second harmonic voltage, $V_{2\omega}$, as a function of the azimuthal
 2 angle, φ , measured at 300 K is shown in Fig. 2(a), which is obtained by
 3 rotating the sample in the XY plane with a fixed external field. $V_{2\omega}$
 4 exhibits a strong dependence on the field: as the applied field increases,
 5 the amplitude of $V_{2\omega}$ weakens. For example, at a low field (50 Oe), a
 6 shoulder like shape around $\varphi = 90^\circ, 270^\circ$ is evident, whereas, at a
 7 relatively high field (350 Oe), $V_{2\omega}$ becomes dependent on $\cos\varphi$ in
 8 addition to the reduced amplitude. By fitting Eq. (3) to the experimental
 9 data, we can separate the second harmonic signal into the dampinglike
 10 and fieldlike contributions, as shown in Fig. 2(b) (f). The black line is
 11 the sum of both dampinglike and fieldlike terms that matches the
 12 experimental data (the green dots) well. The red and blue lines represent
 13 the dampinglike and fieldlike contributions, respectively. The
 14 dampinglike contributions have $\cos\varphi$ dependence and their amplitudes
 15 are all about $0.2\mu V$ at five different fields. The fieldlike contribution
 16 decreases with increasing external field, which is in agreement with the
 17 prediction of Eq. (3).

18 The PHE measurements showed that magnetization is saturated in-
 19 plane at any of the measured fields and that the PHE coefficient, R_p , is
 20 independent of the external field. Hence, the fieldlike torque is inversely
 21 proportional to the external field. Fig. 3(a) shows the fieldlike term in
 22 relation to the external field obtained at different temperatures. It is
 23 found that the external field is much smaller than the demagnetization
 24 field, which is obtained from anomalous Hall effect (AHE)
 25 measurements. It thus follows that, as suggested by Eq. (3), the
 26 dampinglike torque is independent of the external field, as shown in Fig.
 27 3(b). We note, however, that the result measured at 50 K is unexpected.
 28 We take the average of the values obtained at five different external
 29 fields to be the dampinglike torque. To measure the thermal contribution
 30 to the SOTs, we extracted the dampinglike torque also at high fields,
 31 which is shown in the inset of Fig. 3(b). From Eq. (3), we know the
 32 dampinglike torque should vanish at high field. Hence, the intercept
 33 corresponds to infinitely large field at which no dampinglike torque

1 should contribute to the second harmonic voltage. Therefore, the
 2 intercept should reflect the Anomalous Nernst Effect (ANE)
 3 contribution. The linear relation between them and a near zero intercept
 4 shown in Fig. 3(b) indicate clearly that the thermoelectric effect is very
 5 small here.

6 We depict SOTs (fieldlike and dampinglike torque obtained
 7 separated through fitting) as a function of temperature in Fig. 4(a).
 8 Although both types of torque exhibit nearly linear dependence on
 9 temperature, they follow opposite trends, i.e. the dampinglike torque
 10 increases with increasing temperature, whereas the fieldlike torque
 11 decreases with increasing temperature. Using the equation

$$12 \quad \alpha_{DL,FL} = \frac{\tau_{DL,FL}}{J_c} \frac{M_s t_{FM}}{\hbar/2e} \quad (4)$$

13 we calculated the electrical efficiency [26] for 8 nm Cu Au alloy, as
 14 shown in Fig. 4(b). As shown in the figure, α_{DL} increases from 0.0068 at
 15 20 K to 0.0097 at 300 K. This result is comparable with SHA in Au [27].

16 To gain a deeper understanding of the dependence of fieldlike and
 17 dampinglike torque on temperature and to explore the origin of these
 18 two types of torque further, we studied two additional samples with
 19 different NM layer thicknesses. To avoid the difference in current
 20 density caused by resistivity and thickness, we converted the current
 21 density to 10^8 A/cm². We found that the thicker the NM layer, the larger
 22 the SOTs. According to drift diffusion theory [25], the spin current
 23 induced from the bulk spin Hall effect (SHE) is
 24 $J_s(t_N)/J_s(\infty) = 1 - \text{sech}(t_N/\lambda_{sf})$, where t_N is the thickness of the NM layer
 25 and λ_{sf} is the spin diffusion length in the NM layer. Based on this
 26 relation, the spin current increases with the thickness of the NM layer
 27 and saturates only when this thickness reaches the order of the spin
 28 diffusion length. Since the spin diffusion length is around several
 29 hundreds of nanometers in copper and several tens of nanometers in Au
 30 [27,28], the spin diffusion length in CuAu alloy may have the same

1 order of thickness as the NM layer in our samples. A previous study
 2 reported the spin diffusion length in CuAu to be about 5 nm [27]. This
 3 means that the spin current increases but does not saturate within the
 4 range of the sample thickness. In Fig. 5, we plot SOTs as a function of
 5 temperature for samples with different NM layer thickness. The bulk
 6 SHE remains the main source for dampinglike torque given the strong
 7 thickness dependence. Qiu et al. [21] and Kim et al. [22] observed in
 8 Ta/CoFeB/MgO stacks that the fieldlike torque decreased linearly with
 9 decreasing temperature, while the dampinglike torque remained mostly
 10 unaffected. These observations differ from our observations, likely
 11 because in a metal with strong spin orbit coupling, such as Ta and Pt,
 12 intrinsic SHE is the dominant source of SOTs, whereas in our CuAu
 13 samples, extrinsic SHE is the dominant mechanism. With increasing
 14 temperature and thereby increasing scattering events, intrinsic SHE is
 15 not significantly affected and extrinsic SHE increases linearly. Thus, a
 16 different dependence on temperature should be expected. The effective
 17 field of the dampinglike torque linearly increased from ~ 80 120 Oe at 20
 18 K to ~ 170 210 Oe at 300 K. In three samples with different NM layer
 19 thicknesses, the dampinglike torque increased by about 90 Oe as the
 20 temperature varied from 20 K to 300 K. Meanwhile, the fieldlike torque
 21 decreased from ~ 80 100 Oe at 20 K to ~ 50 70 Oe at 300 K.

22 Theoretically, anomalous Hall resistivity in ferromagnetic
 23 materials should scale quadratically or linearly with longitudinal
 24 resistivity (ρ) [29]. The quadratic dependence is posited to come from
 25 the extrinsic side jump or intrinsic mechanism, whereas the linear one
 26 originated from skew scattering. The typically weak dependence of the
 27 metallic resistivity on temperature is presented in Fig. 6(a). Less than 10%
 28 variation in the resistivity, ranging from $26.5 \mu\Omega\cdot\text{cm}$ at 20 K to 29.0
 29 $\mu\Omega\cdot\text{cm}$ at 300 K, is evident. Temperature dependent phonon electron
 30 scattering is thus not the main source of the change in longitudinal
 31 resistivity. Instead, scattering caused by structural disorders in the
 32 CuAu layer may play the dominant role. Fig. 6(b) shows the relation [6]
 33 between α_{DL} and resistivity in our samples. Linear dependence may be

1 the best description of this relation, suggesting that the skew scattering
2 may be the dominant source for the spin Hall effect in these samples.

3 The temperature dependence of the fieldlike torque also deserves
4 some discussion. In Refs. [21] and [22], it is found that in Ta, the
5 fieldlike torque increased with temperature. Within the scenario of
6 interfacial Rashba torque, this increase in fieldlike torque could be
7 attributed to an increase in bulk resistance upon increase in temperature,
8 thereby increasing the current flowing through the interface. This
9 enhancement can therefore be accompanied by an increase in fieldlike
10 torque. In contrast, our experiments show that in CuAu, the fieldlike
11 torque decreases when increasing temperature. Although it is difficult to
12 quantitatively interpret this result, we speculate that Rashba spin orbit
13 coupling is weak at the interface between Au and NiFe [30]. Therefore,
14 in the absence of Rashba spin orbit coupling, a possible origin of the
15 fieldlike torque can be the presence of spin swapping in CuAu, where
16 extrinsic spin orbit scattering dominates the transport. Increasing the
17 temperature would then lead to a decrease in fieldlike torque, as
18 suggested by a recent theory [31]. We emphasize that this explanation
19 remains speculative and requires further experiments to be confirmed.

20 In summary, we used a reliable and convenient method to separate
21 dampinglike torque and fieldlike torque by using experimental data of
22 the harmonic voltage of the transverse resistance. The second harmonic
23 voltage, $V_{2\omega}$, contains two components, the fieldlike and dampinglike
24 terms. The dampinglike term has a $\cos\varphi$ dependence and the fieldlike
25 term has a $2\cos^3\varphi - \cos\varphi$ dependence, which allows us to separate these
26 two contributions by scanning the angle of the in-plane field. This
27 technique is suitable for in-plane magnetized systems while most
28 previous methods can be used only in systems with out of plane
29 magnetization. This method can also be used for out of plane systems
30 only if the external field is strong enough to overcome the perpendicular
31 anisotropy. Importantly, we found that dampinglike torque and fieldlike
32 torque depend on temperature very differently. With increasing
33 temperature, the dampinglike torque increases but the fieldlike torque

1 decreases. The temperature behavior of dampinglike and fieldlike
 2 torque may respectively arise from extrinsic skew scattering and spin
 3 swapping in CuAu alloys. We also found larger SOTs (both dampinglike
 4 torque and fieldlike torque) in samples with thick NM layers.

6 Acknowledgments

7 The research reported in this publication was supported by King
 8 Abdullah University of Science and Technology (KAUST) under CRF
 9 2015 2626 CRG4. The work at University of Delaware was supported
 10 by the U.S. National Science Foundation under DMR grant #1505192.

12 Appendix

13 First, no current is flowing through the stack. In this case, there
 14 exist only two energies: anisotropy energy and Zeeman energy. The total
 15 magnetic energy of this system is thus

$$16 \quad E = -K_{out} \cos^2 \theta - K_{in} \sin^2 \varphi \sin^2 \theta - \vec{M} \cdot \vec{H}, \quad (.4)$$

17 where K_{out} is the effective out of plane anisotropy constant, K_{in} is the
 18 effective in-plane anisotropy constant, θ and φ are the polar and
 19 azimuthal angles of the magnetization moment, \vec{M} . The moment is
 20 defined as

$$21 \quad \vec{M} = M_s \vec{m} = M_s (\cos \varphi_m \sin \theta_m, \sin \varphi_m \sin \theta_m, \cos \theta_m), \quad (.4)$$

22 where M_s is the saturation magnetization and \vec{m} is the unit vector of the
 23 moment. The external field, \vec{H} , is expressed with its polar and azimuthal
 24 angle (θ_H, φ_H) as

$$25 \quad \vec{H} = H (\cos \varphi_H \sin \theta_H, \sin \varphi_H \sin \theta_H, \cos \theta_H). \quad (.4)$$

1 We now consider the relationship between the Hall resistance and the
 2 modulation angle. The Hall resistance typically contains contributions
 3 from the planer Hall effect (PHE) and the anomalous Hall effect (AHE).
 4 Previous reports express the Hall resistance as

$$5 \quad R_H = R_A \cos \theta + R_p \sin^2 \theta \sin 2\varphi , \quad (.4)$$

6 where R_A and R_p are the coefficient of AHE and PHE, respectively. The
 7 current induced field here is small compared with the external field. We
 8 can thus assume that the modulation angle, $\Delta\theta, \Delta\varphi$, is very small. Thus,
 9 we can expand Eq. (A.6) to

$$10 \quad R_H = R_A (\cos \theta_m - \Delta\theta \sin \theta_m) + R_p (\sin^2 \theta_m + \Delta\theta \sin 2\theta_m) (\sin 2\varphi_m + 2\Delta\varphi \cos 2\varphi_m) \quad (.4)$$

11 It turns out that measuring the in-plane external field ($\theta_H = \pi/2$) is
 12 sufficient if samples have large out of plane anisotropy ($|H_K| \gg |\Delta H_Z|$) to
 13 maintain an almost in-plane moment ($\theta_m = \pi/2$). Thus, the Hall resistance
 14 can be simplified to

$$15 \quad R_H = R_p \sin 2\varphi_m + (\Delta\varphi \cdot 2R_p \cos 2\varphi_m - \Delta\theta \cdot R_A) \quad (.4)$$

16 Simultaneously, the modulation angle can be simplified to

$$17 \quad \Delta\theta = \frac{\Delta H_Z}{H_K - H} , \quad (.4)$$

$$18 \quad \Delta\varphi = \frac{-\Delta H_X \sin \varphi_H + \Delta H_Y \cos \varphi_H}{H - H_A} \quad (.4)$$

19 When an alternating current ($i = I \sin \omega t$) is applied, the current induced
 20 field oscillates in the same frequency with the current. We can thus
 21 replace $\Delta\theta, \Delta\varphi$ with $\Delta\theta \sin \omega t, \Delta\varphi \sin \omega t$. Therefore, the Hall voltage can be
 22 expressed as

$$23 \quad V_H = \left[R_p \sin 2\varphi_m \sin \omega t + (\Delta\varphi \cdot 2R_p \cos 2\varphi_m - \Delta\theta \cdot R_A) \sin^2 \omega t \right] I \quad (.4)$$

1 Here, we separate the Hall voltage into three parts determined by the
 2 frequency. The useful parts are the first and second harmonic Hall
 3 voltage, since the zero order part can be easily affected by the DC offset
 4 of the sinusoidal current:

$$5 \quad V_H = V_0 + V_\omega \sin \omega t + V_{2\omega} \cos 2\omega t \quad (.4)$$

$$6 \quad V_\omega = R_p \sin 2\varphi_m \cdot I$$

$$7 \quad V_{2\omega} = -V_0 = \left(-\Delta\varphi \cdot R_p \cos 2\varphi_m + \frac{1}{2} \Delta\theta \cdot R_A \right) I \quad (.4)$$

8 Using Eq. (A.9), Eq. (A.10) and $\varphi \equiv \varphi_m = \varphi_H$, we will have

$$9 \quad V_\omega = R_p \sin 2\varphi \cdot I$$

$$10 \quad V_{2\omega} = \left(\frac{\Delta H_X \sin \varphi - \Delta H_Y \cos \varphi}{H - H_A} \cdot R_p \cos 2\varphi + \frac{1}{2} \frac{\Delta H_Z}{H_K - H} \cdot R_A \right) I \quad (.4)$$

11 To determine fieldlike torque and anti damping torque quantitatively, we
 12 need to use the Landau–Lifshitz–Gilbert equation:

$$13 \quad \frac{d\bar{m}}{dt} = -\gamma \bar{m} \times \left[\bar{H} + \alpha (\bar{m} \times \bar{H}) + H_{FL} \bar{\sigma} + H_{AD} (\bar{m} \times \bar{\sigma}) \right] \quad (.4)$$

14 Here, γ is the gyromagnetic ratio, α is the Gilbert damping coefficient,
 15 \bar{H} is the external field, and $\bar{\sigma}$ is the normalized net spin direction among
 16 the electrons absorbed by the FM layer. $\overline{H_{FL}} = H_{FL} \bar{\sigma}$ and $\overline{H_{DL}} = H_{DL} (\bar{m} \times \bar{\sigma})$
 17 are effective fields induced by fieldlike torque and dampinglike torque,
 18 respectively. Here, for in-plane scan, we have $\bar{m} = (\cos \varphi, \sin \varphi, 0)$ and
 19 $\bar{\sigma} = (0, 1, 0)$, which leads to $\overline{H_{FL}} = (0, H_{FL}, 0)$ and $\overline{H_{DL}} = (0, 0, H_{DL} \cos \varphi)$.

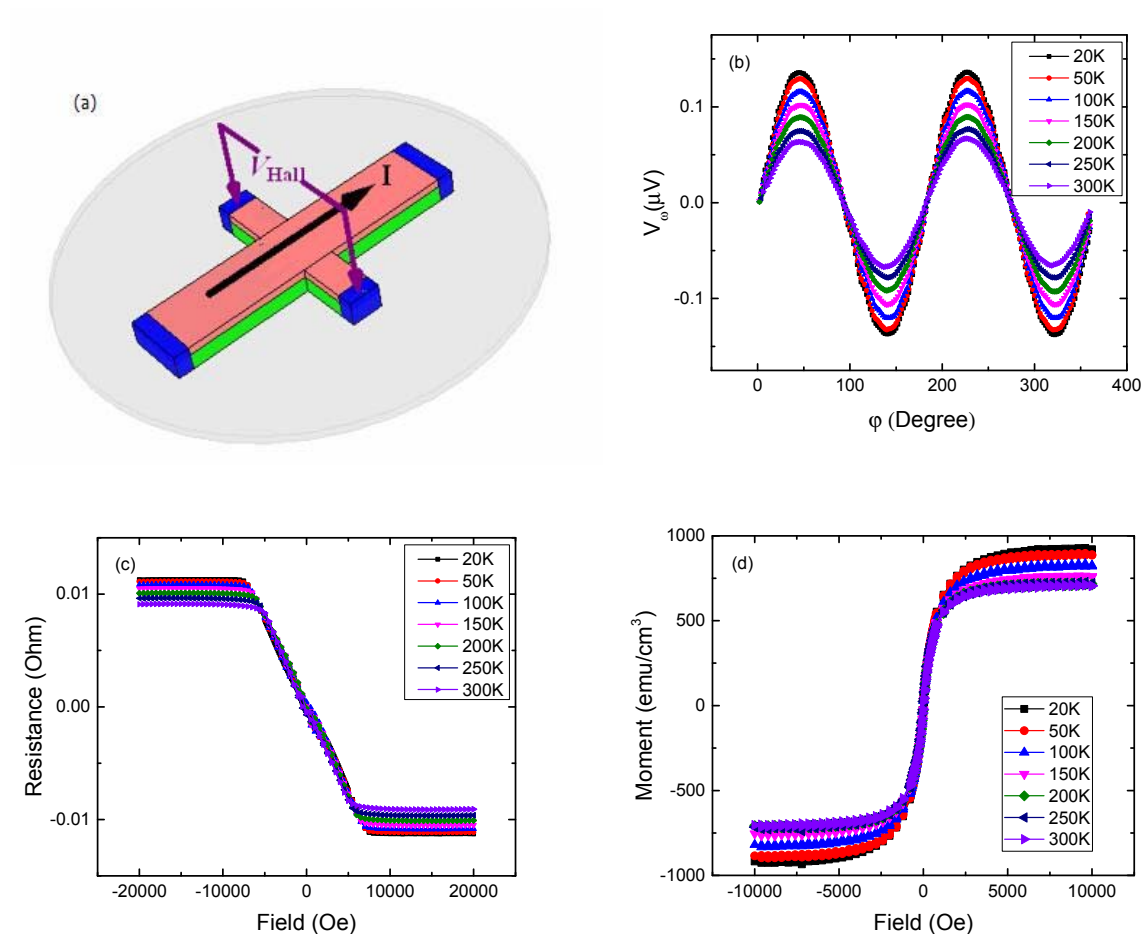
20 Substituting into Eq. (A.14), we have

$$21 \quad V_{2\omega} = \left(\frac{-H_{FL} \cos \varphi}{H - H_A} \cdot R_p \cos 2\varphi + \frac{1}{2} \frac{H_{DL} \cos \varphi}{H_K - H} \cdot R_A \right) I \quad (.4)$$

22 The second harmonic voltage now can be separated by $\cos \varphi$ and
 $2 \cos^3 \varphi - \cos \varphi$ dependence, which corresponds to dampinglike torque
 and fieldlike torque.

References

- 1 [1] T. Jungwirth, J. Wunderlich, and K. Olejnik, *Nature materials* **11**, 382 (2012).
- 2 [2] A. Brataas, A. D. Kent, and H. Ohno, *Nature materials* **11**, 372 (2012).
- 3 [3] F. Matsukura, Y. Tokura, and H. Ohno, *Nature nanotechnology* **10**, 209 (2015).
- 4 [4] P. Gambardella and I. M. Miron, *Philos Trans A Math Phys Eng Sci* **369**, 3175 (2011).
- 5 [5] A. Manchon, H. C. Koo, J. Nitta, S. M. Frolov, and R. A. Duine, *Nature materials* **14**, 871 (2015).
- 6 [6] Q. Hao and G. Xiao, *Physical Review B* **91**, 224413 (2015).
- 7 [7] L. Liu, C. F. Pai, Y. Li, H. W. Tseng, D. C. Ralph, and R. A. Buhrman, *Science* **336**, 555 (2012).
- 8 [8] S. O. Valenzuela and M. Tinkham, *Nature* **442**, 176 (2006).
- 9 [9] I. M. Miron *et al.*, *Nature* **476**, 189 (2011).
- 10 [10] P. M. Haney, H. W. Lee, K. J. Lee, A. Manchon, and M. D. Stiles, *Physical Review B* **87**, 174411
- 11 (2013).
- 12 [11] H. B. M. Saidaoui, Y. Otani, and A. Manchon, *Physical Review B* **92**, 024417 (2015).
- 13 [12] U. H. Pi, K. Won Kim, J. Y. Bae, S. C. Lee, Y. J. Cho, K. S. Kim, and S. Seo, *Applied Physics Letters* **97**,
- 14 162507 (2010).
- 15 [13] J. Kim, J. Sinha, M. Hayashi, M. Yamanouchi, S. Fukami, T. Suzuki, S. Mitani, and H. Ohno, *Nature*
- 16 *materials* **12**, 240 (2013).
- 17 [14] K. Garello *et al.*, *Nature nanotechnology* **8**, 587 (2013).
- 18 [15] C. O. Avci, K. Garello, M. Gabureac, A. Ghosh, A. Fuhrer, S. F. Alvarado, and P. Gambardella,
- 19 *Physical Review B* **90**, 224427 (2014).
- 20 [16] C. O. Avci *et al.*, *Physical Review B* **89**, 214419 (2014).
- 21 [17] M. Hayashi, J. Kim, M. Yamanouchi, and H. Ohno, *Physical Review B* **89**, 144425 (2014).
- 22 [18] M. Jamali, K. Narayanapillai, X. Qiu, L. M. Loong, A. Manchon, and H. Yang, *Phys Rev Lett* **111**,
- 23 246602 (2013).
- 24 [19] X. Fan, J. Wu, Y. Chen, M. J. Jerry, H. Zhang, and J. Q. Xiao, *Nature communications* **4**, 1799
- 25 (2013).
- 26 [20] X. Fan, H. Celik, J. Wu, C. Ni, K. J. Lee, V. O. Lorenz, and J. Q. Xiao, *Nature communications* **5**,
- 27 3042 (2014).
- 28 [21] X. Qiu, P. Deorani, K. Narayanapillai, K. S. Lee, K. J. Lee, H. W. Lee, and H. Yang, *Sci Rep* **4**, 4491
- 29 (2014).
- 30 [22] J. Kim, J. Sinha, S. Mitani, M. Hayashi, S. Takahashi, S. Maekawa, M. Yamanouchi, and H. Ohno,
- 31 *Physical Review B* **89**, 174424 (2014).
- 32 [23] M. Morota, Y. Niimi, K. Ohnishi, D. H. Wei, T. Tanaka, H. Kontani, T. Kimura, and Y. Otani,
- 33 *Physical Review B* **83** (2011).
- 34 [24] T. Tanaka, H. Kontani, M. Naito, T. Naito, D. S. Hirashima, K. Yamada, and J. Inoue, *Physical*
- 35 *Review B* **77** (2008).
- 36 [25] L. Liu, T. Moriyama, D. C. Ralph, and R. A. Buhrman, *Phys Rev Lett* **106**, 036601 (2011).
- 37 [26] H. Li and A. Manchon, *Physical Review B* **93**, 235317 (2016).
- 38 [27] J. Wu, L. Zou, T. Wang, Y. Chen, J. Cai, J. Hu, and J. Xiao, *IEEE Transactions on Magnetics* **52**,
- 39 4100204 (2016).
- 40 [28] M. Isasa, E. Villamor, L. E. Hueso, M. Gradhand, and F. Casanova, *Physical Review B* **91**, 024402
- 41 (2015).
- 42 [29] N. Nagaosa, J. Sinova, S. Onoda, A. H. MacDonald, and N. P. Ong, *Reviews of Modern Physics* **82**,
- 43 1539 (2010).
- 44 [30] S. Grytsyuk, A. Belabbes, P. M. Haney, H. W. Lee, K. J. Lee, M. D. Stiles, U. Schwingenschogl, and
- 45 A. Manchon, *Phys Rev B* **93**, 174421 (2016).
- 46 [31] H. B. Saidaoui and A. Manchon, *Phys Rev Lett* **117**, 036601 (2016).
- 47

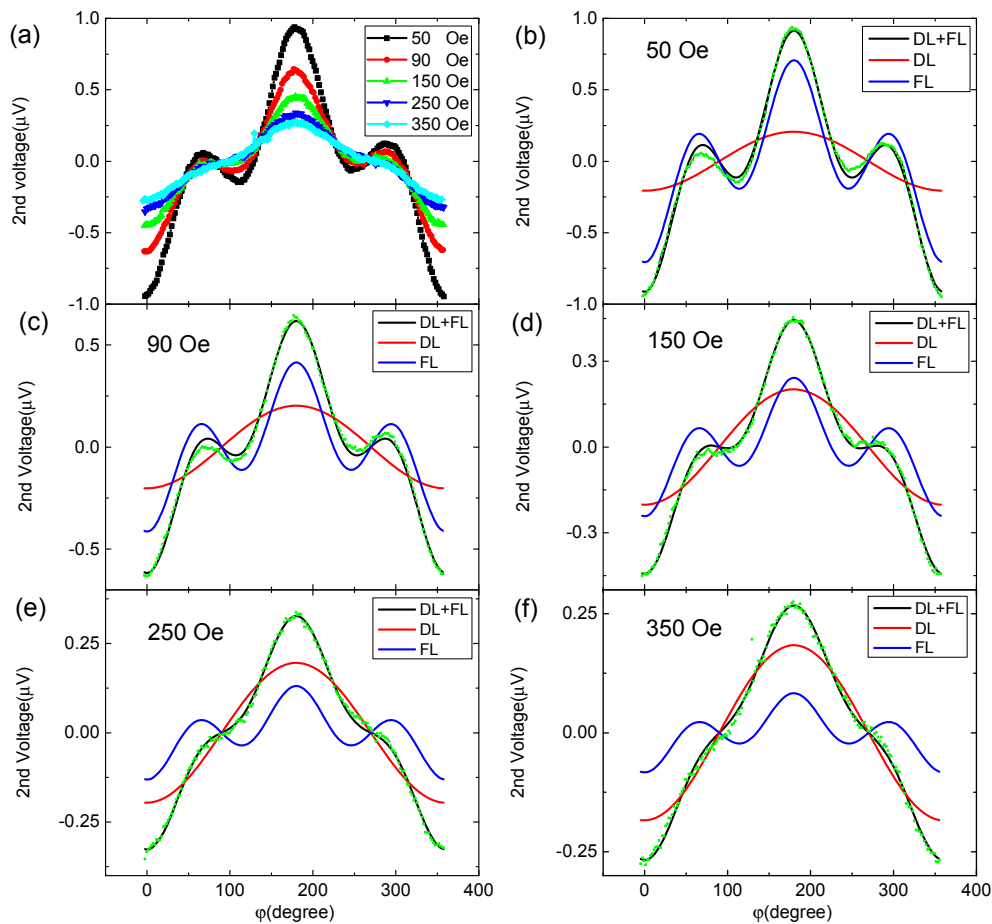


1

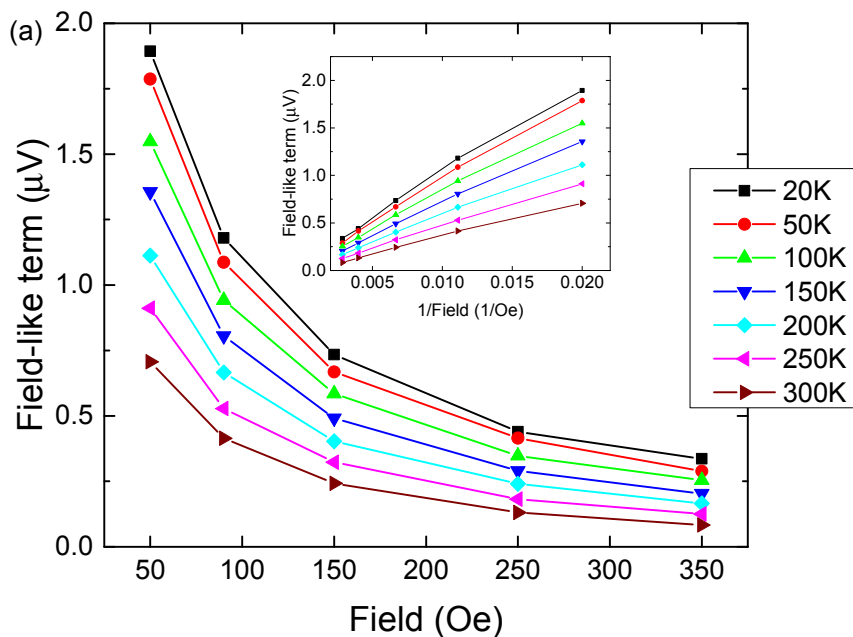
2

3 Figure 1. (a) Schematic of the measurement geometry. (b) The first
 4 harmonic voltage, V_{ω} , as a function of the azimuthal angle, ϕ , (planer
 5 Hall effect) at different temperatures. (c) Anomalous Hall resistance as a
 6 function of the external field measured at various temperatures. (d) The
 7 magnetization curves of NiFe (1.5) as a function of temperature.

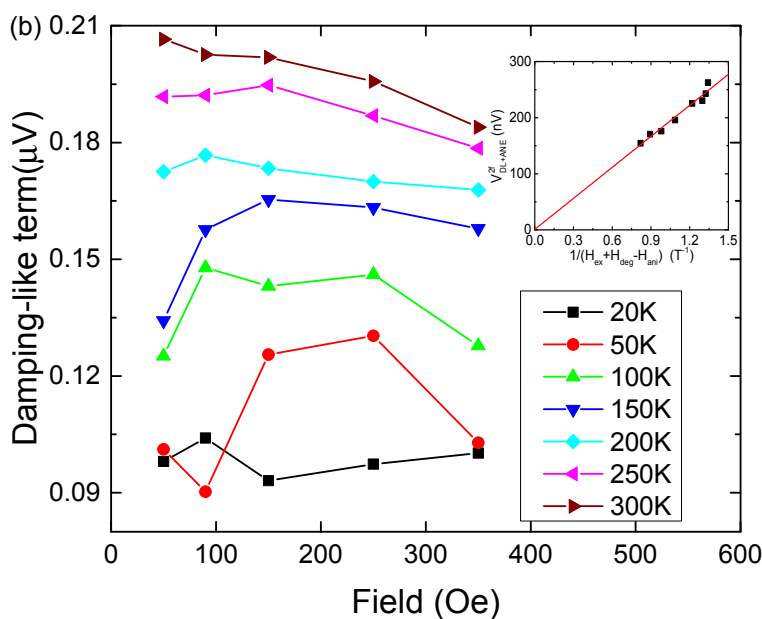
8



1
 2 Figure 2. (a) Second harmonic voltage, $V_{2\omega}$, as a function of the azimuthal
 3 angle, ϕ , measured at 300 K. (b)-(f) Fitting by Eq. (2) from 50 Oe to 350
 4 Oe. The red line is the $\cos \phi$ term, i.e., the dampinglike torque. The blue
 5 line is the $2\cos^3 \phi - \cos \phi$ term, i.e., the fieldlike torque.



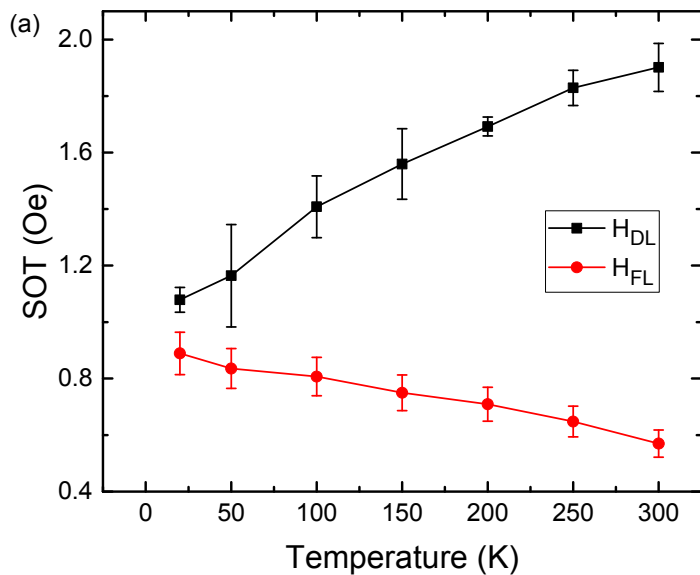
1



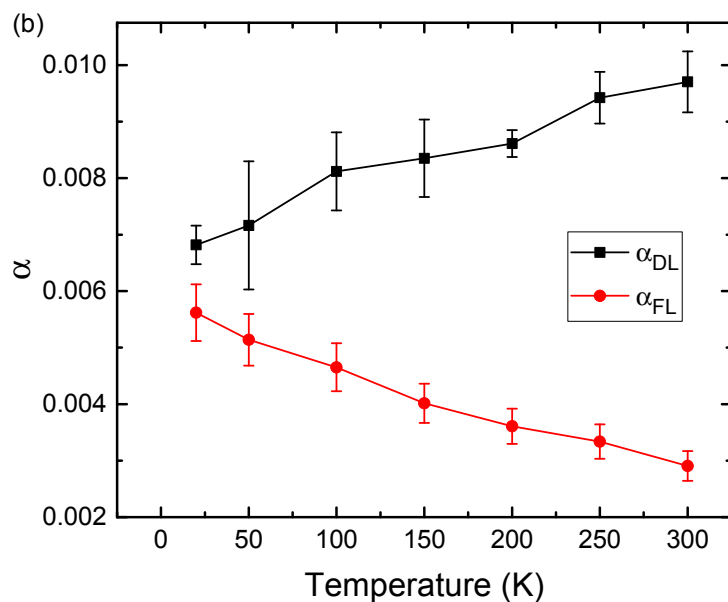
2

3 Figure 3. External field dependence of the extracted (a) fieldlike term
 4 (inset: $1/H$ dependence) and (b) dampinglike term at different
 5 temperatures. (inset: $1/H_{\text{eff}}$ dependence measured at 300 K from 250 Oe
 6 to 5000 Oe.)

7



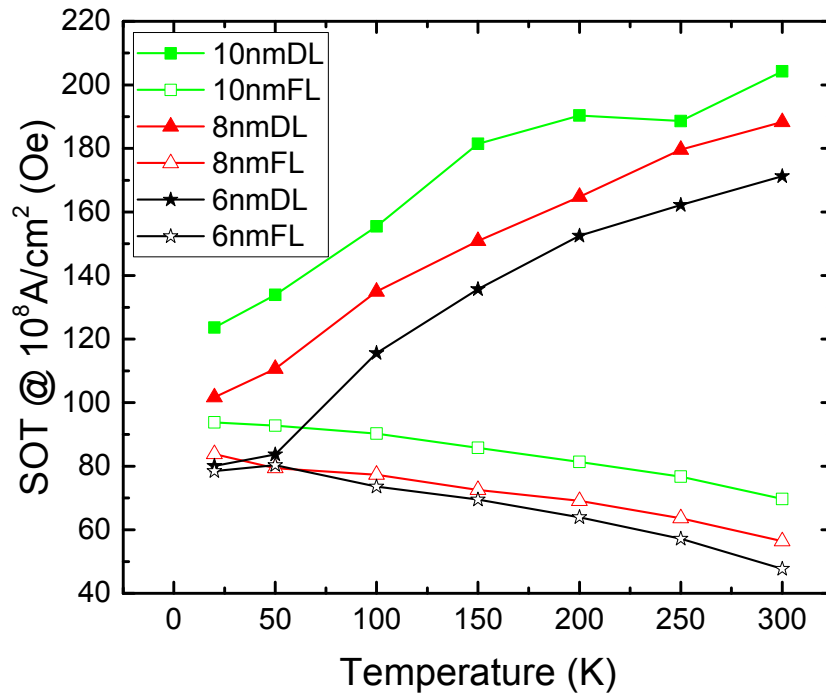
1



2

3 Figure 4. (a) Temperature dependence of the effective field induced by
 4 dampinglike torque and fieldlike torque. (b) Temperature dependence of
 5 the electrical efficiency defined as $\alpha_{DL,FL} = \frac{H_{DL,FL}}{J_c} \frac{M_s t_{FM}}{\hbar/2e}$.

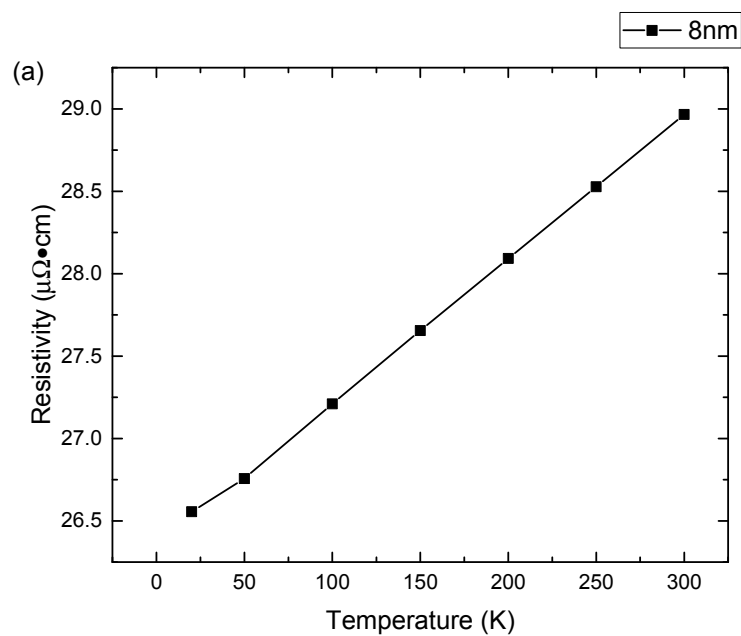
6



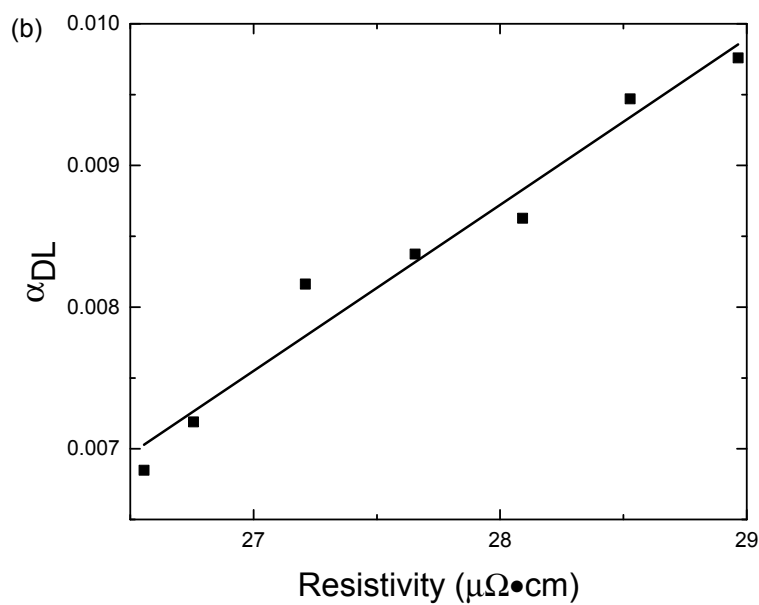
1

2 Figure 5. Thickness dependence of the effective field induced by
 3 dampinglike torque and fieldlike torque. The filled and unfilled symbols
 4 indicate dampinglike and fieldlike torque, respectively. All current
 5 densities are converted to 10^8 A/cm^2 .

6



1



2

3 Figure 6. (a) Resistivity of CuAu (8) as a function of temperature. (b)

4 Relation between α_{DL} and resistivity.

5